Ca^{2+} and cAMP-activated Cl^- conductances mediate Cl^- secretion in a mouse renal inner medullary collecting duct cell line

S. H. Boese, M. Glanville, O. Aziz, M. A. Gray and N. L. Simmons

Department of Physiological Sciences, Medical School, Framlington Place, University of Newcastle upon Tyne, Newcastle upon Tyne NE2 4HH, UK

(Received 21 June 1999; accepted after revision 7 December 1999)

1. The nature of Cl^- conductance(s) participating in transepithelial anion secretion by renal inner medullary collecting duct (IMCD, mIMCD-K2 cell line) was investigated.

2. Extracellular ATP (100 μM) stimulated a transient increase in both whole-cell Cl^- conductance and intracellular free Ca^{2+}. In contrast, ionomycin (10–100 nM) caused a sustained increase in whole-cell Cl^- conductance. Pre-loading cells with the Ca^{2+} buffer BAPTA abolished the ATP-dependent responses and delayed the onset of the increase observed with ionomycin.

3. The Ca^{2+}-activated whole-cell Cl^- current stimulated by ATP (peak) and ionomycin (maximal) displayed (i) a linear steady-state current–voltage relationship and (ii) time and voltage dependence with slow activation at +80 mV and slow inactivation at −80 mV. In BAPTA-loaded cells, ionomycin-elicited whole-cell currents exhibited pronounced outward rectification with time-dependent activation/inactivation.

4. Ca^{2+}-activated and forskolin-activated Cl^- conductances co-exist since ATP activation of whole-cell current occurred during a maximal stimulation by forskolin in single cell recordings.

5. In IMCD epithelial layers, ATP and ionomycin stimulated an inward short circuit current (I_{sc}) dependent upon basal medium Na^+ and Cl^-/HCO_3^- but independent of the presence of apical bathing medium Na^+ and Cl^-/HCO_3^-. This was identical to forskolin stimulation and consistent with transepithelial anion secretion.

6. PCR amplification of reverse-transcribed mRNA using gene-specific primers demonstrated expression of both cystic fibrosis transmembrane conductance regulator (CFTR) mRNA and Ca^{2+}-activated Cl^- channel (mCLCA1) mRNA in mIMCD-K2 cells.

7. Ca^{2+} and forskolin-activated Cl^- conductances participate in anion secretion by IMCD.

The inner medullary collecting duct (IMCD) is capable of significant solute transport and is the final location for determining urinary salt composition (Na^+ and K^+) and acid–base balance. In this segment both electrogenic Na^+ absorption and electrogenic Cl^- secretion (Rocha & Kudo, 1990*a*,*b*; Husted *et al.* 1995, 1998) participate in the regulation of overall NaCl balance. A variety of hormones and paracrines such as atrial natriuretic peptide, vasopressin, nucleotides, prostaglandins and inflammatory cytokines act on this segment (Rocha & Kudo, 1990*a*,*b*; Terada *et al.* 1991; Zeidel, 1993; Husted *et al.* 1995, 1998) to modulate absorptive/secretory processes.

There is now substantial evidence for renal expression of CFTR whose physiological function may include transepithelial Cl^- secretion (Schwiebert *et al.* 1994; Vandorpe *et al.* 1995; Morales *et al.* 1996). CFTR-like channel activity has been shown to be associated with the apical membrane (and transepithelial Cl^- secretion) in both primary cultures of rabbit distal bright convoluted tubule (Poncet *et al.* 1994), M1 collecting duct cells (Letz & Korbmacher, 1997) and in IMCD cell lines (Husted *et al.* 1995). In addition, there is also evidence for renal expression of a novel splice variant of CFTR (Schwiebert *et al.* 1994; Morales *et al.* 1996) which may give rise to functional Cl^- channels. Since the renal deficit in cystic fibrosis is not profound compared with pancreas or small intestine (but see Simmons, 1993, for a discussion of studies of renal deficit in cystic fibrosis patients), alternative mechanisms must exist to compensate for loss of CFTR function (Gray *et al.* 1994; Winpenny *et al.* 1995; King *et al.* 1997). Consideration must be given to the possibility that multiple Cl^- channels are expressed in renal epithelial cells. Molecular techniques have identified a number of Cl^- channels (or Cl^- channel regulators) which show renal expression and where data on specific nephron segmental

patterns of expression may exist. These include CLC Cl^- channels (Uchida *et al.* 1993, 1995; Obermuller *et al.* 1998), pI_{CLn} (a Cl^- channel associated with cell swelling: Paulmichl *et al.* 1992) and more recently a calcium-activated Cl^- channel (mCLCA1/mCaCC) (Gandhi *et al.* 1998; Romio *et al.* 1999). Since a number of stimuli mobilise intracellular Ca^{2+} in IMCD (Zeidel, 1993), the possible expression of a calcium-activated Cl^- channel is of special importance. However, the precise physiological role of such Cl^- channel expression is unresolved (see Schwiebert *et al.* 1994).

IMCD cells that retain significant differentiation *in vitro* have now allowed reconstitution of functional epithelia *in vitro* and the application of patch-clamp studies to study the nature of ion channels in IMCD cells (Sansom *et al.* 1994; Husted *et al.* 1995). Kizer *et al.* (1995) have described an IMCD cell line (mIMCD-K2) established from the initial outer portion of the inner medulla, from a mouse transgenic for SV40. This cell line retains features typical of this segment; for instance a mineralocorticoid-sensitive net Na^+ absorption inhibited by amiloride (Kizer *et al.* 1995) and mediated via apical cyclic nucleotide-gated cation channels (Vandorpe *et al.* 1997). More importantly, this cell line displays electrogenic Cl^- secretion (Kizer *et al.* 1995).

The purpose of the present study was to investigate the nature and regulation of the chloride conductance in the apical membrane of IMCD cells using separate but complementary techniques, namely electrophysiological studies of reconstituted epithelial layers, and the whole-cell configuration of the patch-clamp technique. Furthermore, the possible molecular basis of the apical Cl^- conductance has been investigated by determining specific Cl^- channel mRNA expression in these cells. We present evidence that mIMCD-K2 cells possess two separate apical Cl^- conductances on the basis of the biophysical properties of the activated whole-cell Cl^- conductances and their sensitivity to agents that mobilise intracellular cAMP or Ca^{2+}. Furthermore there is expression of specific mRNAs for both CFTR and mCLCA1 in mIMCD-K2 cells. Preliminary reports of the present data have been presented (Boese *et al.* 1999*a*, *b*).

METHODS

Cell culture

mIMCD-K2 cells (Kizer *et al.* 1995) were a gift from Dr B. Stanton (Dartmouth Medical School, Hanover, NH, USA). mIMCD-K2 cells (18–25 passages) were cultured in Opti-MEM medium supplemented with 5 mM L-glutamine, 50 μg ml^{-1} penicillin–streptomycin and 10% (v/v) fetal bovine serum at 37 °C in an air–5% CO_2 atmosphere. Stock Roux bottles (75 cm^2 growth area) were coated with Vitrogen 100 (purified collagen; Collagen Biomaterials, Palo Alto, CA, USA) and cells were passaged by trypsinisation (2 ml of 0·5% w/v trypsin, 0·7 mM EDTA in Ca^{2+}- and Mg^{2+}-free saline) to form a cell suspension and cultured at a 1:10 split ratio. Epithelial layers of mIMCD-K2 cells were prepared by seeding (2×10^5 cells cm^{-2}) onto Vitrogen 100-coated permeable filter supports (Snapwell, Costar, Corning Inc., Corning, NY, USA; 12 mm diameter, 0·4 μm pore diameter) and incubated for up to 14 days with medium replacement every 2–3 days. For patch-clamp/intracellular Ca^{2+} measurements cells were seeded at 1×10^4 cells per coverslip (25 mm diameter) and cultured as above.

Measurements of short-circuit current and epithelial resistance

Epithelial layers were mounted in an Ussing chamber at 37 °C, connected to an automatic voltage clamp (WPI, DVC-1000, New Haven, CT, USA) and measurements of open-circuit potential difference, transepithelial resistance (R_t) and short-circuit current (I_{sc}) were made (Simmons, 1992) in Krebs solution.

Whole-cell patch-clamp analysis

mIMCD-K2 cells on coverslips were superfused at 5 ml min^{-1} (volume of tubing and switch ~1 ml, chamber volume ~0·5 ml) at room temperature whilst membrane currents were measured using the nystatin slow whole-cell configuration of the patch-clamp technique (Hamill *et al.* 1981). Borosilicate patch pipettes had resistances, after fire polishing, of 3–6 MΩ. Seal resistances were between 5 and 20 GΩ. Whole-cell currents were measured with an EPC9 patch-clamp amplifier (HEKA, Lambrecht, Germany) at a holding potential of 0 mV with excursions to ±80 mV. Data were filtered at 1 kHz and sampled at 2 kHz. The slope conductance was obtained by linear regression of the mean current values at 0·5–1·0 s averaged from voltage steps (held for 1 s) to +80 and −80 mV in 20 mV increments. Reversal potentials were determined from voltage ramps from −80 to +80 mV. In the standard bath and pipette solutions cell capacitance was 23·4 ± 2·6 pF and the membrane potential was −24·9 ± 1·0 mV ($n = 99$).

Measurements of intracellular Ca^{2+}

mIMCD-K2 cells on coverslips were incubated with 5 μM fura-2 AM in growth media for 35–50 min at 37 °C, in a 5% CO_2–95% air atmosphere, washed 3 times in bathing solution (see below) before the coverslip was imaged using an oil immersion lens (Nikon, Fluor 40 n.a. 1·3), and superfused (volume of tubing and switch ~1 ml, bath volume 0·5 ml, perfusion at 2 ml min^{-1}). Changes in intracellular Ca^{2+} were determined by measuring the ratio of fluorescence (520 long pass filter) of fura-2-loaded cells (group of 3–5) with dual wavelength (alternate 340 and 380 nm) excitation (Life Science Resources Microspectrofluorimeter, Cambridge, UK). Data were corrected for background but not cell autofluorescence.

Determination of expression of CFTR and mCLCA1 mRNA transcripts by reverse transcription-polymerase chain reaction

The basic method for isolation of poly-A^+ RNA from cultured cells (mIMCD-K2, T84) based on detergent lysis, digestion of RNases with proteinase K and affinity separation on oligo-dT resin has been described previously (Walker *et al.* 1998). Mice were killed by cervical dislocation, their kidneys obtained and rapidly frozen in liquid nitrogen. Total RNA was then isolated by acid–phenol extraction of solubilised tissue (RNAzol B, Biogenesis, Poole, Dorset, UK). Poly-A^+ RNA was then purified using oligo-dT resin as above. The quantity of mRNA was assessed by absorbance at 260 nm, the quality was assessed by the ratio of absorbance at 260 nm over that at 280 nm ($A_{260\ nm/280\ nm}$). Poly-A^+ RNA (1 μg) was reverse transcribed using Moloney murine leukaemia virus reverse transcriptase (M-MuLV RT, MBI Fermentas) and random hexanucleotide primers in a standard reaction (Thwaites *et al.* 1999). Omission of M-MuLV RT provided a negative control for DNA contamination. PCR reactions were performed over 30 cycles at 2 mM $MgCl_2$ using recombinant *Taq* DNA polymerase (MBI Fermentas). Each cycle consisted of 94 °C for 30 s, 54 °C or 55 °C (CFTR or mCLCA1, respectively) for 30 s, and 72 °C for 1 min. Oligonucleotide primers for CFTR isoforms (Morales *et al.* 1996)

were: forward primer 5′-AAAAAAGGAAGAATTCTATTCT-3′, reverse primer 5′-CTAAGCACCAAATTAGCAC-3′, and allow detection of full-length and truncated CFTR isoforms (Morales *et al.* 1996). Oligonucleotide primers for mCLCA1 (mCaCC) were: forward primer 5′-GCCTCCATAATGTTCATGC-3′, reverse primer, 5′-CCGGAAGTGCTCGGTCAC-3′ (Gruber *et al.* 1998). PCR products were analysed using agarose gel electrophoresis–ethidium bromide fluorescence, purified (QIA gel extraction kit (Qiagen, Crawley, Sussex, UK)) and cloned using the TA cloning vector pCR2.1 TOPO (Invitrogen, Groningen, The Netherlands). Cloned PCR products were sequenced using fluorescent di-deoxy dye-termination on an ABI Prism model 377 automated sequencer. Comparison of cloned PCR fragments to published sequence was performed using BLASTN (www.ncbi.nlm.nih.gov) (Altschul *et al.* 1997).

Solutions

The Krebs solution used for I_{sc} measurements contained (in mmol l^{-1}): NaCl, 125; KCl, 5·4; $CaCl_2$, 2·8; $MgSO_4$, 1·2; KH_2PO_4, 1·5; $NaHCO_3$, 20; glucose, 5 (pH 7·4 at 37 °C) gassed continuously with 95% O_2–5% CO_2. A Na^+-free solution was prepared by replacement of NaCl and $NaHCO_3$ with their respective choline salts. A Cl^-- and HCO_3^--free medium was obtained by replacement of NaCl, $NaHCO_3$ and KCl with their gluconate salts and buffering with Tris-Hepes (10), pH 7·4. For patch-clamp and intracellular

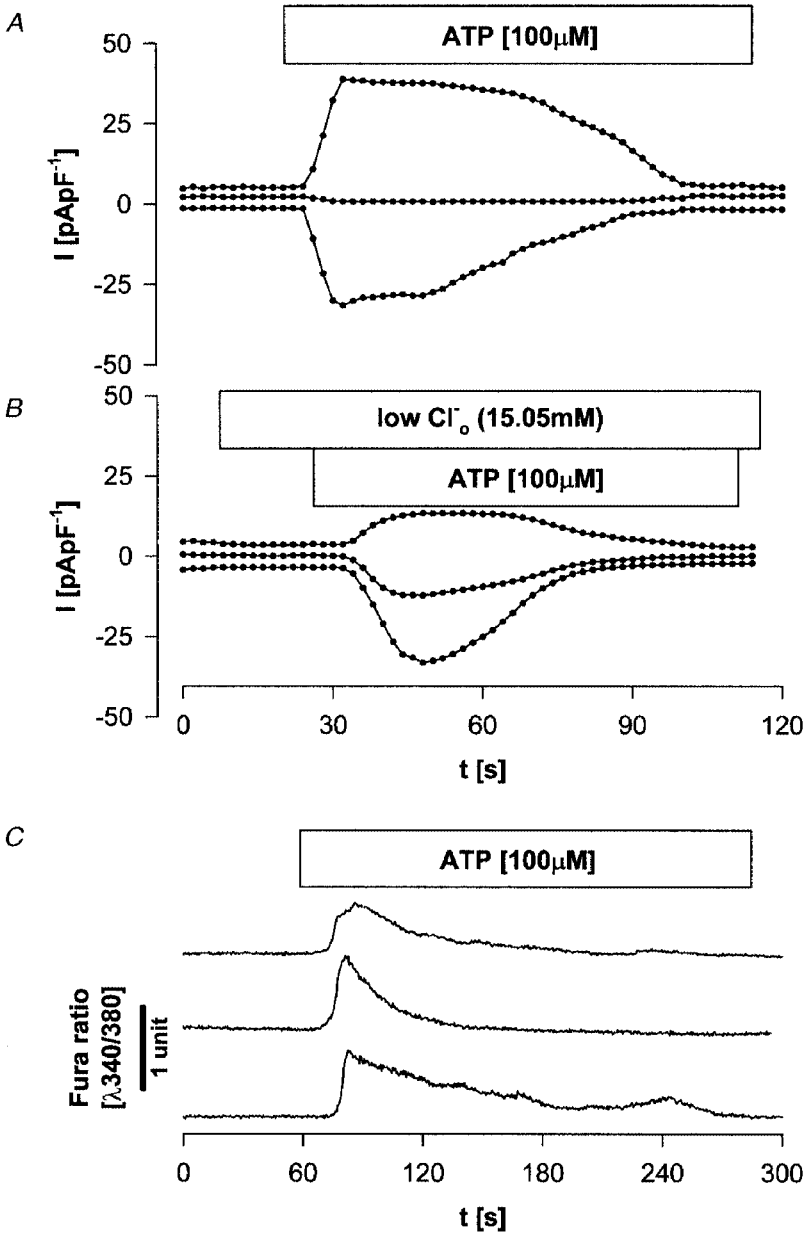

Figure 1. Stimulation of whole-cell current and intracellular Ca^{2+} by exogenous ATP

A, stimulation of whole-cell current by exogenous ATP (100 μM) in mIMCD-K2 cells in the standard bath solution. Data are shown for the membrane potential held at 0 mV (200 ms) and alternated at ±80 mV for 500 ms every 2 s. *B*, stimulation of whole-cell current by exogenous ATP (100 μM) when bath Cl^- was reduced 10-fold. Other details as for *A*. *C*, stimulation of intracellular Ca^{2+} by ATP (100 μM). Cells in standard bath solution were superfused with ATP-containing solution. Intracellular Ca^{2+} is expressed as the ratio of emissions at 340 nm/380 nm; records are displaced to show 3 separate experiments.

Ca^{2+} recordings the bath solution contained (in mmol l^{-1}): NaCl, 140; KCl, 4·5; KH_2PO_4, 1; $MgCl_2$, 1; $CaCl_2$, 2; Hepes, 10; tris(hydroxymethyl)aminomethane (Tris), ~6; glucose, 5; pH 7·4. A 10-fold reduction in [Cl^-] was obtained by replacement of NaCl with sodium aspartate. For patch clamp bath solutions were hypertonic (320 mosmol l^{-1}) with 20 mM sucrose to obviate activation of swelling-sensitive currents (Boese *et al.* 1996). The pipette solution (300 mosmol l^{-1}) contained (in mmol l^{-1}): NaCl, 10; KCl, 130; $MgCl_2$, 2; Hepes, 10; Tris ~5; and nystatin (100–200 μg ml^{-1}); pH 7·2.

Materials

4,4′-Diisothiocyanatostilbene-2,2′-disulphonic acid (DIDS) (Pflatz and Bauer, New York, USA) was dissolved (10^{-2} M) in dimethylsulphoxide (DMSO) and diluted to give a final bath concentration of 10–500 μM. DMSO at the concentrations used was without effect. Forskolin and ionomycin (Sigma Chemical Co., Poole, Dorset, UK) were dissolved in ethanol (10^{-2} M) and used at 10 and 0·1–1 μM (respectively). Benzamil (Tocris, Bristol, UK) was dissolved in Krebs solution at 1 mM and used at a concentration of 50 μM. ATP was made as a stock solution of the Na^+ salt in Krebs solution. BAPTA-AM and fura-2 AM were from Molecular Probes Inc., OR, USA. Culture media and other chemicals used were from Sigma.

Statistics

Data are expressed as mean values ± S.E.M. for n separate epithelial layers or cells. Significance of difference between mean values was determined using ANOVA with Bonferroni corrections for multiple comparisons applied to Student's t test (unpaired data) for tests between individual data pairs (where appropriate). The level of significance was set at $P \leqslant 0{\cdot}05$.

RESULTS

ATP stimulation of whole-cell currents in mIMCD-K2 cells

Figure 1*A* shows that ATP stimulates a rapid increase in whole-cell currents (time to peak after inflection was 19 ± 3 s ($n = 20$). The increase was transient, declining to pre-stimulation levels 111 ± 11 s after peak values. Basal whole-cell slope conductances (±80 mV, see Methods) of 121·0 ± 22·4 pS pF^{-1} increased to 716 ± 91·5 pS pF^{-1} at peak ($P < 0{\cdot}05$ *vs.* control), with currents then declining to 133 ± 24 pS pF^{-1} after 3 min (n.s. *vs.* control). With the membrane potential held at 0 mV, cell activation by ATP was associated with a decrease in the small outward whole-cell current towards zero (Fig. 1*A*). These data are consistent with ATP activation of a Cl^- conductance. In order to confirm this, the Cl^- in the standard bath solution was reduced 10-fold using aspartate replacement. Basal conductance was only slightly reduced (Fig. 1*B*, mean data, to 105 ± 35 pS pF^{-1}, $n = 8$, n.s. *vs.* control data above) whilst ATP-stimulated outward currents (peak values) at +80 mV were markedly reduced from 60·1 ± 8·0 to 18·9 ± 2·5 pA pF^{-1} ($n = 8$, $P < 0{\cdot}05$). As expected for activation of a Cl^- conductance, ATP addition caused an increase in inward whole-cell current with the membrane potential held at 0 mV (Fig. 1*B*). Inward current at −80 mV was maintained (at peak values plus 100 μM ATP, −55 ± 6·6 pA pF^{-1}, $n = 8$, compared with standard bath solution,

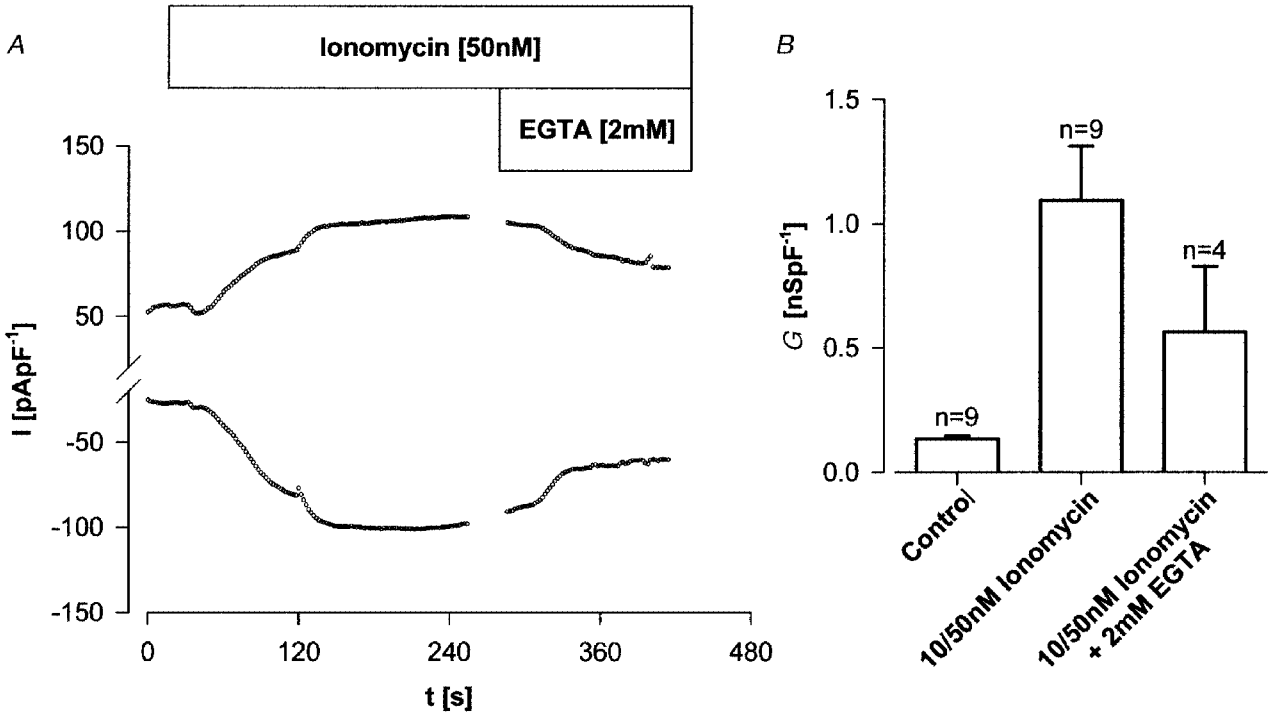

Figure 2. Ionomycin stimulation of whole-cell current

A, stimulation of whole-cell current (I) by ionomycin (50 nM). In the standard bath solution a progressive increase in whole-cell current to a plateau was partially reversed with superfusion of an EGTA (2 mM)-containing bath solution. Membrane potential was held at 0 mV for 200 ms and alternated to ±80 mV for 500 ms. *B*, summary of whole-cell conductances (G) for basal, ionomycin and ionomycin after superfusion with 2 mM EGTA-containing bath solution.

$-51 \pm 1{\cdot}0$ pA pF^{-1}, n.s.). The major effect of ATP is therefore to activate whole-cell Cl^- conductance.

In order to test whether a purinoreceptor-coupled mobilisation of intracellular Ca^{2+} (Ecelberger *et al.* 1994; Brown *et al.* 1995) was responsible for activation of the whole-cell Cl^- conductance, fura-2-loaded mIMCD-K2 cells were superfused with ATP. Figure 1*C* shows that 100 μM ATP stimulated a rapid increase (time to peak after inflection was 24 ± 9 s ($n = 8$; not significantly different from the increase in whole-cell Cl^- conductance, $P > 0{\cdot}05$) in intracellular Ca^{2+} whose duration (time for return to baseline after peak was 133 ± 21 s, $n = 8$) was not significantly different from that seen for the change in whole-cell Cl^- conductance. In four separate experiments the ratio at 340 nm/380 nm was increased from $0{\cdot}6 \pm 0{\cdot}1$ to $1{\cdot}5 \pm 0{\cdot}15$ at the peak of the response to ATP.

Ionomycin stimulation of whole-cell currents in mIMCD-K2 cells

Figure 2*A* shows that the Ca^{2+} ionophore ionomycin (10–50 nM) also activated whole-cell currents. In contrast to the ATP-mediated increase in whole-cell Cl^- conductance, the ionomycin-activated conductance was maintained and was only partially reversed when bath Ca^{2+} was chelated with 2 mM EGTA ($P < 0{\cdot}01$, paired data). Figure 2*B* shows that the mean increase in whole-cell conductance with ionomycin was approximately 7-fold (control slope conductance $134 \pm 11{\cdot}2$ pS pF^{-1}, $n = 9$; plus ionomycin $1094{\cdot}0 \pm 217{\cdot}9$ pS pF^{-1}, $n = 9$, $P < 0{\cdot}05$). When the standard bath solution was changed to one containing a reduced $[Cl^-]$ (as for ATP stimulation, aspartate replacement) basal conductance was unaffected ($218 \pm 82{\cdot}1$ pS pF^{-1}, $n = 4$, n.s. *vs.* controls); however, the ionomycin-stimulated (50 nM) outward currents (maintained values) at +80 mV were markedly reduced from $101 \pm 2{\cdot}8$ to $44 \pm 3{\cdot}6$ pA pF^{-1} ($n = 4$; $P < 0{\cdot}05$). There was a concurrent shift in reversal potential in a positive direction (by $20{\cdot}6 \pm 1{\cdot}6$ mV, $n = 8$) during external anion replacement. Inward current at −80 mV plus ionomycin was, in contrast, maintained ($-82 \pm 7{\cdot}7$ pA pF^{-1}, $n = 4$) compared with standard bath solution ($-80 \pm 10{\cdot}8$ pA pF^{-1}, $n = 4$, n.s.). When iodide or bromide replacements were made instead of aspartate for ionomycin-stimulated cells the ratio of conductances (G_{anion}/G_{Cl}) at +80 mV was I^- (1·7) > Br^- (1·4) > Cl^- (1·0) (mean data $n = 4$ for I^- and Br^-). A similar sequence was evident from the change in reversal potential when NaCl was completely replaced with NaI or NaBr; I^- (shift of $-13 \pm 0{\cdot}9$ mV *vs.* Cl^-, $n = 3$) > Br^- ($-2{\cdot}2 \pm 0{\cdot}8$ mV,

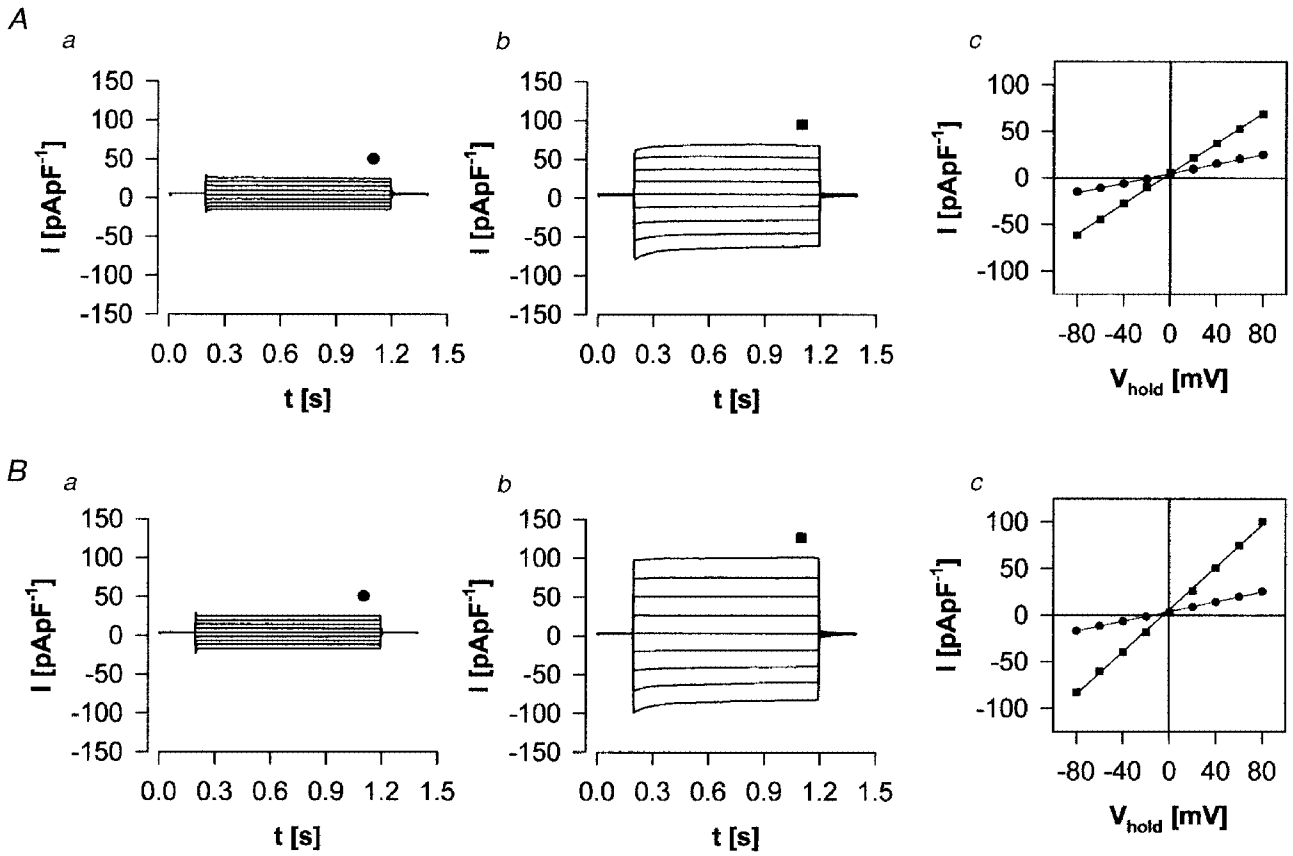

Figure 3. Biophysical characteristics of stimulated whole-cell currents

Biophysical characteristics of whole-cell currents stimulated by ATP (100 μM; *A*) and by ionomycin (100 nM; *B*) in mIMCD-K2 cells. *Aa*, basal; *Ab*, at peak stimulation by 100 μM ATP; *Ac*, *I–V* relationship of control (●) and ATP (■) data at ~1 s following voltage step (indicated in *Aa* and *Ab*). *Ba*, *b* and *c*, as in *A* but with ionomycin instead of ATP. Cell was held at 0 mV and pulsed to voltages between ±80 mV for 1 s.

$n = 3$) ≈ Cl^-. Thus, as with ATP stimulation, the ionomycin data are consistent with the existence of a Ca^{2+}-activated Cl^- conductance in mIMCD-K2 cells.

Biophysical properties of the Ca^{2+}-activated Cl^- conductance

Figure 3 compares the biophysical characteristics of basal whole-cell currents (Fig. 3*Aa* and *Ba*) with those stimulated by ATP (100 μM, Fig. 3*Ab*) and ionomycin (100 nM, Fig. 3*Bb*) in mIMCD-K2 cells at peak values. Basal currents were time independent and showed a linear *I–V* relationship. As noted above replacement of bath Cl^- by aspartate had only minimal effects on whole-cell conductance and the ionic basis of basal currents was not investigated further. Both ATP and ionomycin stimulated significant increases in whole-cell current of 5·9- and 8·2-fold, respectively. In contrast to basal currents, stimulated currents displayed time- and voltage-dependent kinetics with slow activation during depolarisation and slow inactivation during hyperpolarisation (Fig. 3*A* and *B*). At steady state (~1 s) linear current–voltage (*I–V*) relationships were observed for both ATP and ionomycin conditions.

ATP and ionomycin stimulation of whole-cell currents in BAPTA-loaded mIMCD-K2 cells

Figure 4*A* shows the effect of ATP and ionomycin upon free $[Ca^{2+}]_i$ after prolonged BAPTA loading. Whereas the ATP-stimulated transient increase in Ca^{2+} was abolished, the ionomycin-dependent increase was delayed by 5–10 min. ATP-stimulated whole-cell currents were abolished in BAPTA-loaded cells (whole-cell slope conductance was 119 ± 55 pS pF^{-1}, $n = 8$; plus ATP at 1 min, conductance was 154 ± 43 pS pF^{-1}, n.s.), whereas with ionomycin there was a prolonged delay followed by an increase of whole-cell current (Fig. 4*B*). Figure 4*C* shows that the biophysical characteristics of the Ca^{2+}-activated whole-cell Cl^- current depended upon the level of $[Ca^{2+}]_i$ attained; the kinetics of the stimulated current clearly showed marked outward rectification with time-dependent activation/inactivation at intermediate levels of whole-cell current and at intermediate Ca^{2+} levels (Fig. 4*Cc*). This dependence of kinetics upon $[Ca^{2+}]_i$ is similar to that described for Ca^{2+}-activated whole-cell Cl^- conductance by Evans & Marty (1986) and Winpenny *et al.* (1998).

Forskolin-activated currents co-exist with Ca^{2+}-activated Cl^- currents in mIMCD-K2 cells

Figure 5*A* shows the effect of forskolin upon whole-cell currents in mIMCD-K2 cells. Forskolin (10 μM) increased basal conductance from $124 \pm 26{\cdot}4$ pS pF^{-1} to a maintained value of $269 \pm 28{\cdot}5$ pS pF^{-1} ($n = 6$, $P < 0{\cdot}05$). In contrast to ATP and ionomycin, forskolin-stimulated whole-cell currents were time independent and the *I–V* relationship was linear. These results are typical for CFTR and substantiate the observations of Vandorpe *et al.* (1995) who examined 8-(4-chlorophenyl-thio)adenosine 3′,5′-cyclicmonophosphate (CPT-cAMP) stimulation of whole-cell currents using the fast whole-cell patch configuration.

Figure 5*B* shows the co-existence of ATP and forskolin-stimulated currents within a single mIMCD-K2 cell. After the transient stimulation achieved with ATP (peak change in current with ATP, $-20{\cdot}6 \pm 0{\cdot}1$ pA pF^{-1}, $n = 4$, at a holding potential of −30 mV), forskolin resulted in a maintained stimulation ($-6{\cdot}4 \pm 0{\cdot}4$ pA pF^{-1}, $n = 4$) to which subsequent addition of ATP produced a further transient stimulation (to $-16{\cdot}2 \pm 0{\cdot}5$ pA pF^{-1} above the forskolin level). The effect of ATP in the presence of concurrent forskolin stimulation showed a small but significant reduction compared with ATP alone (above, $P < 0{\cdot}05$).

A pharmacological distinction may also be made between Ca^{2+}-activated and forskolin-activated Cl^- currents; in the presence of 500 μM DIDS, ionomycin-stimulated whole-cell currents were reduced to $43{\cdot}8 \pm 3{\cdot}1$% ($n = 4$) of control values whereas forskolin-stimulated currents were unaffected ($n = 4$).

Location and physiological role for the Ca^{2+}-activated Cl^- channel in mIMCD-K2 cells

In order to investigate the physiological role of the Ca^{2+}-activated Cl^- channel in epithelial monolayers of mIMCD-K2 cells we have investigated the effect of Ca^{2+}-mobilising stimuli upon anion-dependent inward I_{sc} in voltage-clamped epithelial monolayers in Ussing chambers. In 25 representative layers mean transepithelial resistance was $1326 \pm 208\ \Omega\ cm^2$. whilst basal I_{sc} was minimal at $1{\cdot}3 \pm 0{\cdot}19\ \mu A\ cm^{-2}$. These values are similar to those described by Kizer *et al.* (1995). The levels of I_{sc} electrogenic Na^+ absorption in these layers is therefore negligible, since epithelial monolayers are cultured in the absence of mineralocorticoids (Kizer *et al.* 1995). In confirmation, apical benzamil (50 μM) reduced basal I_{sc} by ~25%.

Addition of 100 μM ATP to either apical or basal bathing solution stimulated a transient increase in inward I_{sc} to peak values at ~1 min of $8{\cdot}1 \pm 2{\cdot}1$ and $5{\cdot}6 \pm 2{\cdot}2\ \mu A\ cm^{-2}$, respectively. At 3 min post-stimulation the increase compared with baseline values had declined to $3{\cdot}5 \pm 1{\cdot}1$ and $0{\cdot}9 \pm 0{\cdot}8\ \mu A\ cm^{-2}$, respectively. The transient nature of the I_{sc} response to ATP corresponds to the time course of the ATP-stimulated increase in both intracellular Ca^{2+} and whole-cell Cl^- conductance (see above). That this increase represents basal to apical anion secretion was confirmed by the data in Table 1, which demonstrate that the ATP-stimulated inward I_{sc} was neither inhibited by apical benzamil nor when apical Na^+ was replaced with choline. Furthermore, ATP-stimulated I_{sc} was not inhibited when apical bathing solution Cl^-/HCO_3^- content was replaced with gluconate. In contrast, when basal Na^+ was replaced with choline or when Cl^-/HCO_3^- content was replaced with gluconate, the ATP-stimulated inward I_{sc} was abolished. Application of 0·1 or 1 μM ionomycin to the apical bathing solution also resulted in stimulation of inward I_{sc}, but in contrast to ATP, a maintained plateau phase was observed (Fig. 6). Application of excess EGTA (2 mM) during the plateau phase reversed the ionomycin-dependent increase in

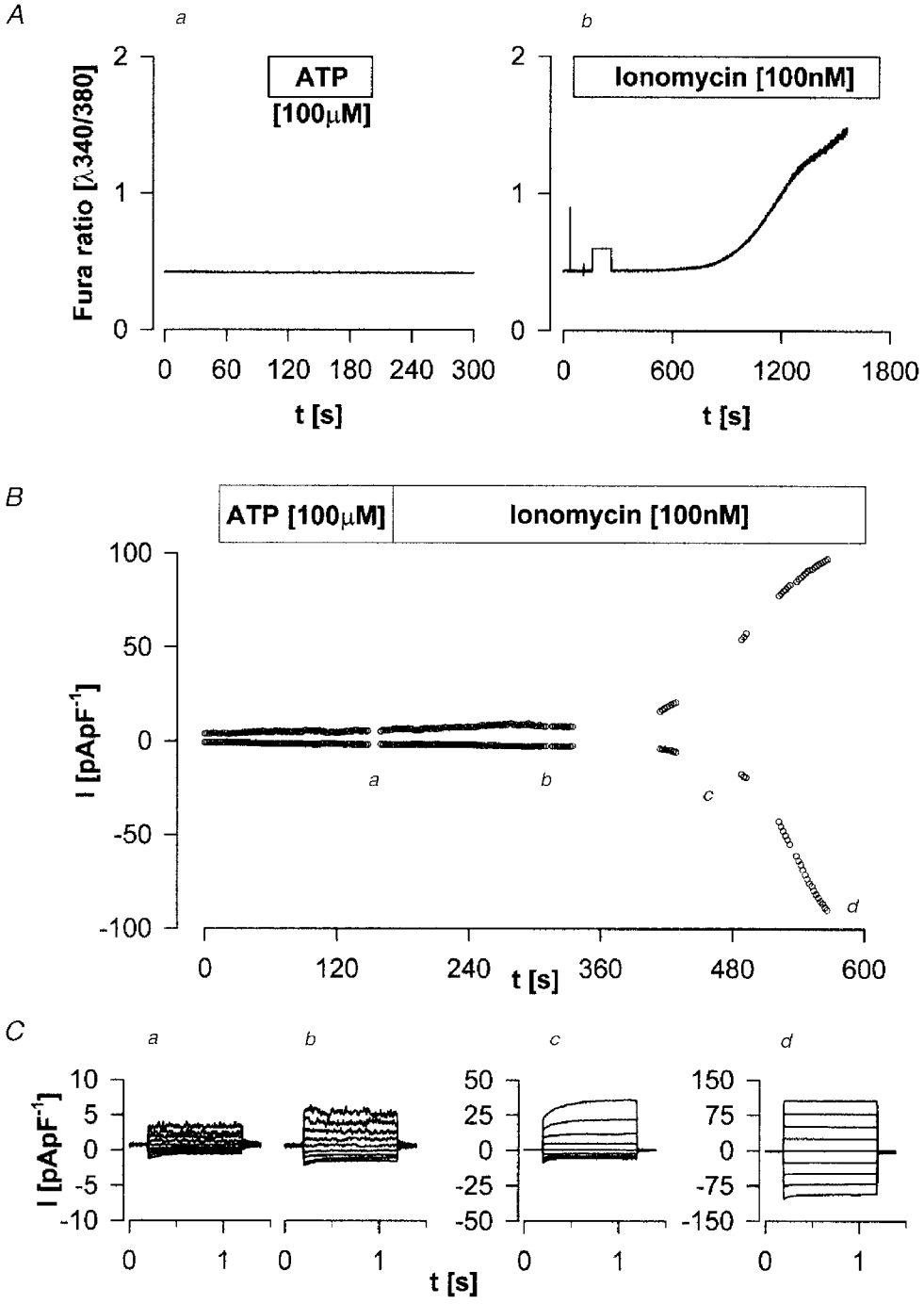

Figure 4. Effect of BAPTA loading upon Ca^{2+}-dependent activation of whole-cell conductances and a change in intracellular Ca^{2+} in mIMCD-K2 cells

A, $[Ca^{2+}]_i$ in cells grown on coverslips (see Methods) loaded with 5 μM fura-2 AM together with 30 μM BAPTA-AM for 60 min prior to measurement. *a*, cells superfused with standard bath solution and then exposed to 100 μM ATP failed to show normal Ca_i^{2+} transient (representative of 3). *b*, exposure to 100 nM ionomycin in standard bath solution showed only a limited change in $[Ca^{2+}]_i$ up to 10 min but thereafter there was a progressive increase in $[Ca^{2+}]_i$. *B*, whole-cell currents at $\pm$80 mV in cells preloaded with BAPTA-AM. Cells were preloaded with 30 μM BAPTA-AM for 60 min and then superfused with standard bath solution during whole-cell recording. Stimulation by ATP (*a*) was without effect (representative of 4 experiments). There was a progressive increase in whole-cell current upon continued exposure to 100 nM ionomycin (*b–d*). *C*, biophysical characteristics of whole-cell currents at various times (*a–d* in *B*) in BAPTA-loaded cells. Cell was held at 0 mV and pulsed to voltages between $\pm$80 mV for 1 s. Note the marked outward rectification in *c* and that the time-dependent activation/inactivation of current during voltage pulses depended on $[Ca^{2+}]_i$, this being especially evident in *c*.

I_{sc} (from $3{\cdot}2 \pm 0{\cdot}4$ to $0{\cdot}0 \pm 0{\cdot}2\ \mu A\ cm^{-2}$, $n = 5$). The ionomycin-stimulated increase in I_{sc} displayed an identical ion dependency to that observed for ATP stimulation (Table 1), consistent with basal to apical anion secretion. Comparison of ATP/ionomycin stimulation to forskolin stimulation of CFTR (Table 1) shows that the Na^+ and anion dependence of forskolin-stimulated I_{sc} was identical to that observed for ATP and ionomycin. The ability of both ATP and ionomycin to stimulate anion secretion via increased cytosolic Ca^{2+} is consistent with the apical location of the Ca^{2+}-activated Cl^- conductance observed in whole-cell patch-clamp recordings (see above). A basolateral location of the Ca^{2+}-activated Cl^- conductance would in contrast short-circuit secretion stimulated via apical CFTR by enhancing futile cycling across the basolateral membrane (Simmons, 1991). Accordingly the effect of ionomycin ($0{\cdot}1\ \mu M$) was tested alone and in combination with $10\ \mu M$ forskolin. After stimulation with forskolin ($8{\cdot}9 \pm 1{\cdot}5\ \mu A\ cm^{-2}$, $n = 5$), ionomycin addition gave a further (peak) stimulation ($1{\cdot}5 \pm 0{\cdot}6\ \mu A\ cm^{-2}$) of inward I_{sc}. This suggests that both Ca^{2+}-activated and cAMP-activated Cl^- channels are present at the apical membrane. Addition of ionomycin alone gave a stimulation significantly greater than that after forskolin ($7{\cdot}5 \pm 1{\cdot}5\ \mu A\ cm^{-2}$, $n = 5$, paired data $P < 0{\cdot}05$).

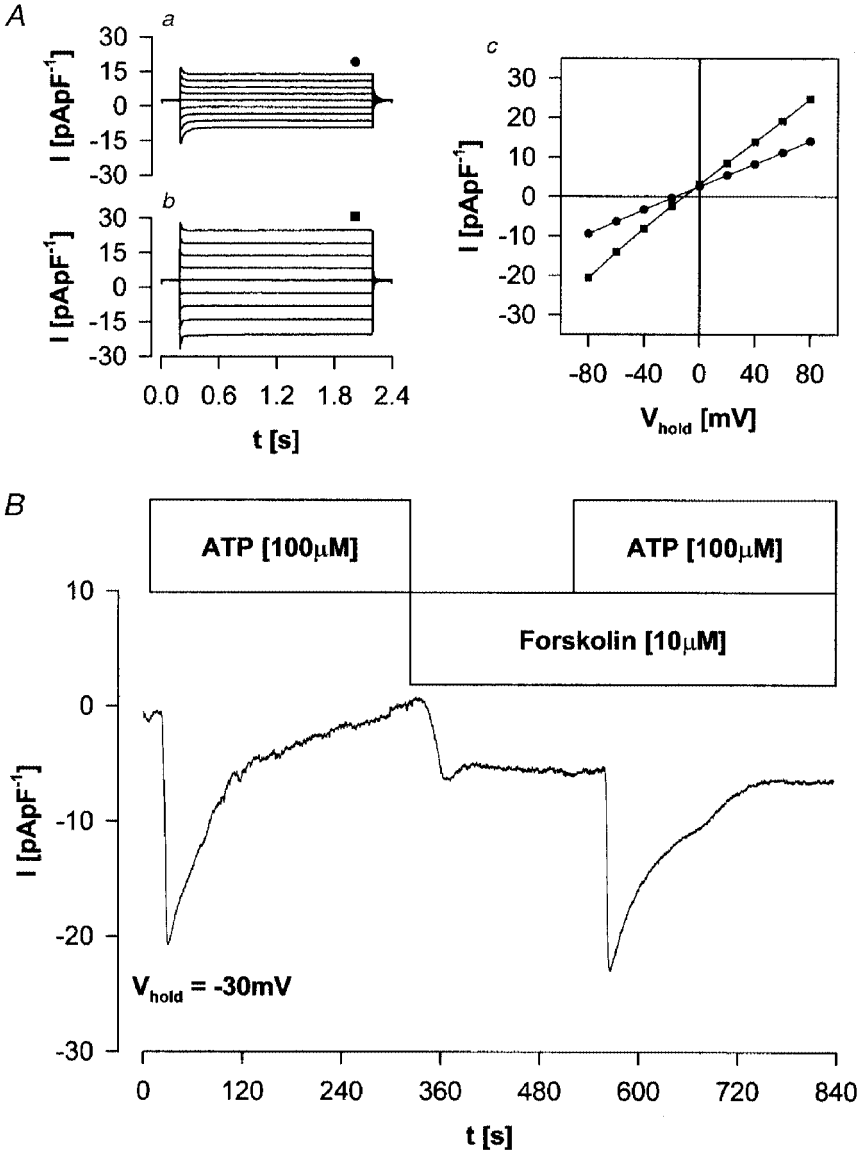

Figure 5. Forskolin-activated whole-cell currents

A, forskolin-activated whole-cell currents in mIMCD-K2 cells. *a*, representative traces of basal current; *b*, representative traces of forskolin-activated ($10\ \mu M$) current. Cells were held at 0 mV and pulsed between ± 80 mV in 20 mV steps. *c*, *I–V* diagram of control (●) and forskolin-activated (■) currents at ~1·5 s as indicated in *a* and *b*. *B*, co-existence of ATP and forskolin-stimulated currents in mIMCD-K2 cells. Representative trace where cell was held at −30 mV and superfused with standard bath solution containing ATP ($100\ \mu M$) and forskolin ($10\ \mu M$), alone and in combination. Note the maintained stimulation of current by forskolin and the additive effect of ATP.

Forskolin (10 μM) addition at the plateau of the ionomycin response gave a further stimulation ($3{\cdot}7 \pm 0{\cdot}9$ μA cm^{-2}, $n = 5$) but this was significantly smaller than that with forskolin alone ($P < 0{\cdot}05$, not shown). The maintained levels of secretion with both agents present ($10{\cdot}2 \pm 1{\cdot}1$ μA cm^{-2}) did not differ significantly from the (peak) levels observed for ionomycin or forskolin alone. This contrasts with the synergism usually observed in Cl^--secretory systems expressing CFTR such as MDCK epithelia (Simmons, 1992).

As with whole-cell currents ionomycin- and forskolin-stimulated currents may be distinguished pharmacologically; DIDS (500 μM) added to the apical medium reduced ionomycin-stimulated levels of I_{sc} to $21{\cdot}7 \pm 11{\cdot}3$% ($n = 6$) of the maintained levels. This concentration was without effect upon forskolin-stimulated I_{sc} ($n = 4$).

Co-expression of mClCA1 and CFTR mRNA in mIMCD-K2 cell line

We have utilised an RT-PCR approach to demonstrate expression of mCLCA1 (mCaCC) mRNA in IMCD cells. Using gene-specific primers (Gruber *et al.* 1998) to amplify reverse-transcribed mRNA, a major PCR product of ~518 bp was identified in whole kidney as well as in

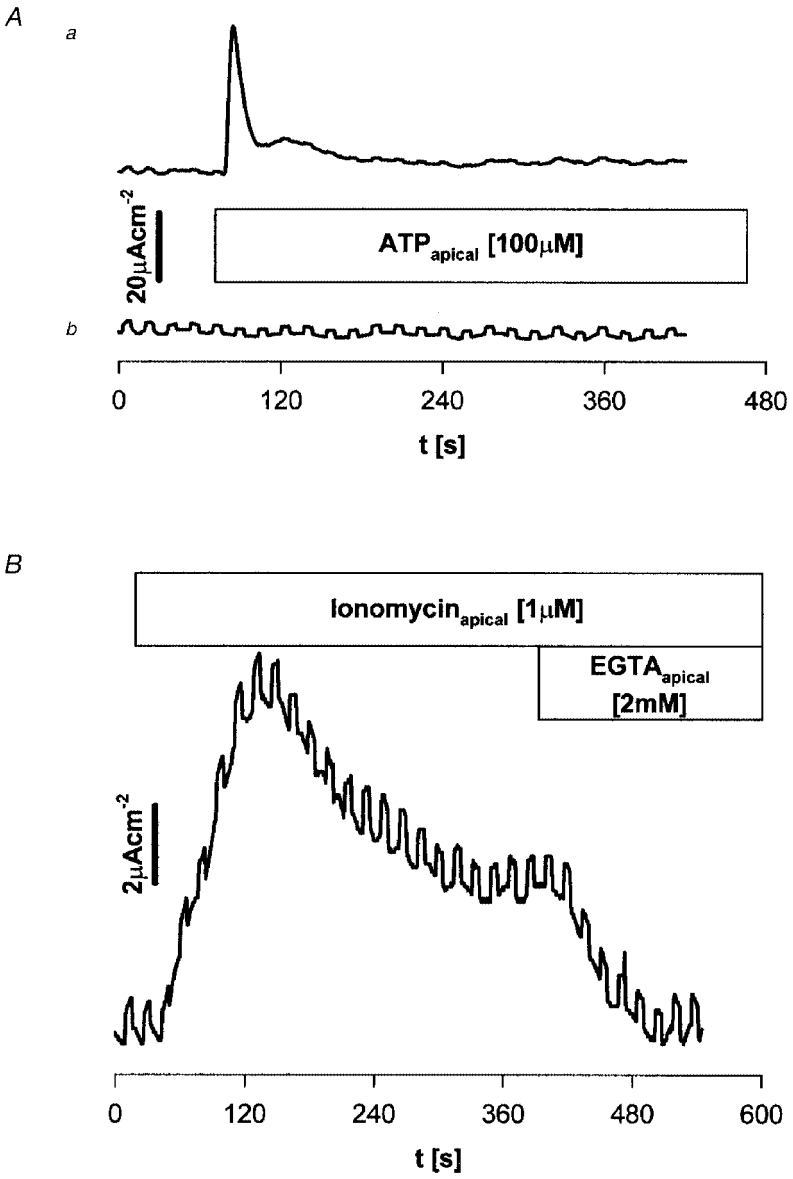

Figure 6. Measurement of inward I_{sc} in reconstituted mIMCD-K2 epithelial layers

A, representative traces showing the effect of apical addition of 100 μM ATP upon inward I_{sc} (upward deflection) in asymmetric bathing solutions; upper trace has the apical bathing solution Cl^-/HCO_3^- free. Lower trace has the basal bathing solution Cl^-/HCO_3^- free. Data are representative of 4 monolayers. Upward deflections represent excursions of the voltage clamp by +0·5 mV. *B*, representative trace showing the effect of 1 μM ionomycin added to the apical solution on inward I_{sc} in Krebs solution. At the plateau 2 mM EGTA was added to the apical bathing solution. Note the prompt reversal towards pre-stimulation levels.

Table 1. Ion dependency of inward I_{sc} stimulated by ATP, ionomycin and forskolin

Condition	ATP	Ionomycin	Forskolin
Krebs solution	8·15 ± 2·1 (10)	8·25 ± 0·7 (11)	10·65 ± 1·3 (6)
50 μM benzamil	20·5 ± 4·4 (4)	9·4 ± 1·4 (4)	—
Na^+ free (a)	17·4 ± 5·1 (3)	9·1 ± 2·8 (3)	12·6 ± 1·2 (3)
Na^+ free (b)	n.r. (3)	0·2 ± 0·2 (3)	n.r. (3)
Cl^-/HCO_3^- free (a)	21·9 ± 4·25 (4)	4·75 ± 0·6 (4)	11·75 ± 0·9 (4)
Cl^-/HCO_3^- free (b)	n.r. (4)	−0·6 ± 0·3 (5)	n.r. (4)

All values are in $\mu A\ cm^{-2}$. Ion replacements were made in the apical (a) or basal (b) bathing solution. Extracellular ATP (0·1 mM) and ionomycin (0·1 and 1 μM, pooled data) were added to the apical solution. Forskolin (10 μM) was added to the basal bathing solution. Values in parentheses are the number of separate monolayers used in each condition. n.r., no response detected. —, not done.

mIMCD-K2 epithelial cells (Fig. 7*A*) consistent with mCLCA1 (mCaCC) mRNA expression (Gandhi *et al.* 1998; Romio *et al.* 1999). This result cannot arise due to genomic DNA contamination since on omission of reverse transcriptase, a PCR product was not evident in either the whole kidney or mIMCD-K2 samples. Cloning and sequencing of the PCR product in both forward and reverse orientations (clone 550/6 from mIMCD-K2 cells) further confirmed identity to mCaCC/mCLCA1 (accession numbers, AF047838, Gandhi *et al.* 1998; U36445, Romio *et al.* 1999; 96% identity, 510/518 bp, no gaps, Altschul *et al.* 1997).

Co-expression of CFTR mRNA together with mCaCC mRNA in the mIMCD-K2 cell line was confirmed by amplification of a 510 bp PCR product using gene-specific primers for CFTR (Fig. 7*B*). T84 cells were included as a positive control. Since the primer design allows for detection of both the full-length (510 bp) and alternatively spliced truncated CFTR isoform (365 bp) (Morales *et al.* 1996), it seems likely that only full-length wild-type CFTR is expressed in mIMCD-K2 cells (Vandorpe *et al.* 1995).

DISCUSSION

The collecting duct system (cortical collecting duct (CCD), outer medullary collecting duct (OMCD) and inner medullary collecting duct (IMCD)) is both morphologically and physiologically heterogeneous. Clapp *et al.* (1989) have arbitrarily separated the inner medullary collecting tubule into three portions, namely the outer, middle and inner portions (IMCD1, 2 and 3, respectively). IMCD1 may be considered to be a continuation of the OMCD whilst IMCD2 and IMCD3 display a morphologically homogeneous cell population which have similar physiological characteristics and are termed the terminal portion of the IMCD ($IMCD_t$).

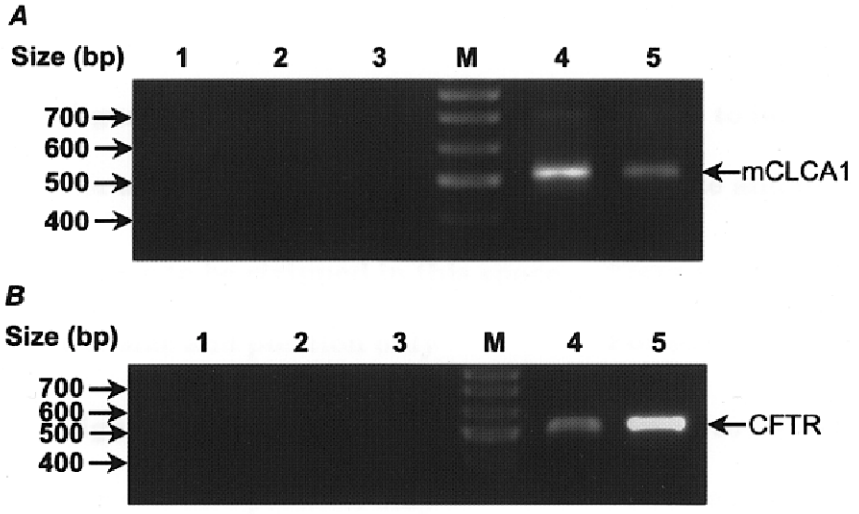

Figure 7. Ethidium-stained agarose gel showing RT-PCR products

A, mCLCA1 gene-specific primers. Lane 1, PCR control (water alone); lanes 2 and 3, controls omitting reverse transcriptase for mIMCD-K2 and mouse kidney mRNA samples; M, molecular size ladder; lane 4, mIMCD-K2 cell line; lane 5, positive control mouse kidney. *B*, CFTR gene-specific primers. Lane 1, PCR control; lanes 2 and 3, minus reverse transcriptase controls for mIMCD-K2 and T84; M, molecular size ladder; lane 4, mIMCD-K2 cell line; lane 5, positive control, T84 cell line.

The cell line used in the present study was originally isolated from the initial half of the inner medulla from mice transgenic for SV40 from cells and established by clonal dilution (Kizer *et al.* 1995). The basic transport characteristics of reconstituted mIMCD-K2 epithelia used in this study have been extensively characterised: an electrogenic apical to basal Na^+ absorption stimulated by mineralocorticoids and sensitive to inhibition by amiloride and by atrial natriuretic hormone (Kizer *et al.* 1995; Green *et al.* 1996). A cyclic nucleotide-gated cation channel has been identified by whole-cell patch-clamp analysis to mediate apical Na^+ entry in mIMCD-K2 cells (Vandorpe *et al.* 1997). In addition to Na^+ absorption, mIMCD-K2 cells display transepithelial anion secretion stimulated by arginine vasopressin via cAMP (Kizer *et al.* 1995). Anion secretion in mIMCD-K2 cells involves uphill accumulation of Cl^-/HCO_3^- across the basolateral membrane followed by downhill movement across the apical membrane. The nature of the apical Cl^- exit pathway has been studied by Vandorpe *et al.* (1995) who demonstrated CPT-cAMP activated whole-cell currents consistent with CFTR. In addition, CFTR mRNA was identified using an RT-PCR approach. In this study we confirm the basic epithelial properties found by Kizer *et al.* (1995), the stimulation of whole-cell Cl^- currents by cAMP (forskolin) and the expression of full-length CFTR mRNA (Morales *et al.* 1996). The phenomenon of anion secretion in IMCD has been documented both in primary cultures of rat inner medullary cells where electrogenic Na^+ absorption occurs together with Cl^- secretion (Husted *et al.* 1995, 1998) and in isolated microdissected, microperfused IMCD (Rocha & Kudo, 1990*a*, *b*). It seems likely that mIMCD-K2 epithelia therefore represent a useful model system to explore the physiology of the outer IMCD.

Properties of the Ca^{2+}-activated Cl^- conductance in mIMCD-K2 cells

The evidence that a Ca^{2+}-activated Cl^- conductance exists in mIMCD-K2 cells is 4-fold. First, agonists such as ATP that cause transient mobilisation of intracellular Ca^{2+}, activate Cl^--selective whole-cell currents with a similar time course. Second, ionomycin causes a sustained increase in intracellular Ca^{2+} and also causes a sustained activation of Cl^--selective whole-cell currents. Ionomycin-stimulated whole-cell Cl^- currents are partially reversed upon Ca^{2+} chelation of the external bathing solution. Third, increasing intracellular Ca^{2+} buffer capacity by pre-loading cells with BAPTA abolishes the ATP-dependent increase in intracellular Ca^{2+} and the activation of whole-cell currents. Finally, BAPTA treatment delays the onset of the ionomycin-stimulated whole-cell currents as well as the increase in intracellular Ca^{2+}. The magnitude of the Ca^{2+}-activated Cl^- conductance is greater/comparable to that observed for cAMP-activated Cl^- conductance (CFTR); basal currents are increased approximately 9-fold (to 1·09 nS pF^{-1}) by ionomycin. These values are also similar to Ca^{2+}-activated Cl^--activated Cl^- conductances observed in mouse pancreatic duct cells where this conductance may be the primary route for Cl^- secretion across the apical membrane (Gray *et al.* 1994; Winpenny *et al.* 1995). The characteristics of the Ca^{2+}-activated whole-cell Cl^- current stimulated by either ATP or ionomycin were (1) a linear current–voltage relationship at steady state, and (2) time and voltage dependence with slow activation during depolarisation and slow inactivation during hyper-polarisation. It should be noted that the biophysical characteristics of the Ca^{2+}-activated whole-cell Cl^- currents depend upon the level of $[Ca_i^{2+}]$ attained. In ionomycin treatment with BAPTA loading, the kinetics of the stimulated current clearly show marked outward rectification with time-dependent activation/inactivation (Fig. 4*Bc*). This dependence of kinetics of Ca^{2+}-activated whole-cell Cl^- conductance upon $[Ca^{2+}]_i$ has been described by Evans & Marty (1986) who noted that at 0·5 μM internal Ca^{2+}, large relaxations in current amplitude were observed and that the *I–V* relationship was markedly rectifying, whereas at 2·0 μM Ca^{2+}, relaxations were of smaller magnitude and the *I–V* relationship was virtually linear (Evans & Marty, 1986). The anion selectivity of the Ca^{2+}-activated whole-cell Cl^- conductance was determined during ionomycin stimulation as $I^- > Br^- > Cl^-$, similar to Eisenman sequence 1 as described by Evans & Marty (1986).

Cl^- currents stimulated by cAMP are also observed in mIMCD-K2 cells (and are likely to result from CFTR expression; see above). These currents show a linear *I–V* relationship but time and voltage independence and so are readily distinguished from those activated by Ca^{2+}. The selectivity for CPT-cAMP Cl^- currents in mIMCD-K2 cells is $Cl^- = Br^- > I^-$ (Vandorpe *et al.* 1995) and is therefore distinct from Ca^{2+}-activated currents (see above). Finally the Ca^{2+}-activated whole-cell Cl^- current is sensitive to block by DIDS whereas the forskolin-stimulated Cl^- current is not.

A key observation from the whole-cell recordings is that both Ca^{2+}-activated and forskolin-activated Cl^- conductances co-exist in the same cells since additive activations of whole-cell current are observed with a maximal stimulation by forskolin together with ATP. Thus mIMCD-K2 cells are similar to other secretory cells (Anderson & Welsh, 1991). This observation also argues against the possibility that an intermediate (e.g. prostaglandin) is involved in stimulation by ATP so activating CFTR-Cl^- currents.

Molecular identity of whole-cell Cl^- currents

Cunningham *et al.* (1995) were the first to describe a full-length bovine cDNA encoding an epithelial (lung) Cl^- channel that encodes an ionomycin-stimulated Cl^- conductance when transfected into transformed monkey kidney (COS) cells. Using homology cloning Gandhi *et al.* (1998) further identified a mouse homolog (mCLCA1) from a mouse lung cDNA library. Northern analysis has revealed expression of mCLCA1 in heart, lung, liver and kidney. The analysis of the tissue distribution of mCLCA1 was investigated further by Gruber *et al.* (1998) by *in situ* hybridisation, RT-PCR

analyses and Northern blotting. mCLCA1 was strongly expressed in mouse secretory tissue such as mammary gland, respiratory and intestinal epithelia, but also in other epithelial tissue including kidney, uterus and epididymis. Independently using database BLAST searches Romio *et al.* (1999) identified a mouse EST clone containing a full-length open reading frame (mCaCC) homologous to bovine calcium-activated Cl^- channel and virtually identical to that described by Gandhi *et al.* (1998) at the nucleotide level. Northern analysis indicated a restricted expression to skin and kidney. Using the mCLCA1 primers as described by Gruber *et al.* (1998), we show expression of mCLCA1 mRNA in mIMCD-K2 cells. Gruber *et al.* indicated that 'tubular epithelial cells' expressed the mCLCA1 product; our results suggest that it is likely that inner medullary collecting duct cells express mCLCA1.

The functional properties of cloned mCLCA1 have been investigated by heterologous expression in human embryonic kidney (HEK) cells (Gandhi *et al.* 1998) and in *Xenopus* oocytes (mCaCC, Romio *et al.* 1999). In HEK cells, calcium-dependent currents were activated by inclusion of 2 mM Ca^{2+} in the pipette during 'fast' whole-cell patch-clamp recording, or by ionomycin treatment. These Ca^{2+}-activated Cl^- currents were outwardly rectifying, but time independent, showing no activation on depolarisation or inactivation on hyperpolarisation. In *Xenopus* oocytes, in the absence of ionophore, mCaCC expression was associated with elevation of an outwardly rectifying time-independent Cl^- current. DIDS inhibited the currents conferred by mCLCA1/mCaCC expression. The properties of the cloned mCLCA1/mCaCC are thus similar but not identical to the biophysical properties of the calcium-activated Cl^- current in mIMCD-K2 cells. This diversity in properties may arise due to the different cellular context in which expression occurs. However, it is known that at least two glycosylated protein products are processed from the initial protein precursor (Gandhi *et al.* 1998) and that mCLCA1 is but one of a family of related proteins. This suggests the possibility that the properties conferred by homomeric mCLCA1/mCaCC may be different to that observed in native tissues where heteromeric associations are possible. Finally, since a significant Cl^- conductance is observed in transfected oocytes without mobilisation of intracellular calcium (Romio *et al.* 1999), different regulatory pathways may exist in native tissues.

Physiological role of Cl^- currents in mIMCD-K2 cells

What is the physiological role of the Ca^{2+}-activated Cl^- currents identified in this study in mIMCD-K2 cells? The evidence presented from reconstituted epithelial layers where both ATP and ionomycin stimulate anion-dependent I_{sc} demonstrate that the Ca^{2+}-activated Cl^- conductance is present at the apical membrane and participates in trans-epithelial anion secretion. It is thus likely that a wide variety of hormones and paracrines can activate apical Cl^- conductance via mobilisation of intracellular Ca^{2+}. ATP may act at both epithelial surfaces in IMCD to stimulate inward I_{sc}, most probably at the apical surface via a $P2_u$ receptor mechanism (Brown *et al.* 1995). Possible agonists include nucleotides such as ATP, UTP, kinins, acetylcholine, adrenaline/noradrenaline and inflammatory cytokines (Zeidel, 1993; Simmons, 1993; Ecelberger *et al.* 1994; Husted *et al.* 1998).

Husted & Stokes (1996) have stressed that the IMCD can both actively absorb Na^+ and secrete Cl^- suggesting that overall NaCl transport is achieved by a balance between these two processes. Since secretory current flow depends on medium HCO_3^- levels (Husted *et al.* 1995), a proportion of the current may represent HCO_3^- secretion. Clearly the direction of anion flow in the IMCD depends on the electrochemical gradient for Cl^- or HCO_3^- across the apical membrane. Even in the presence of significant trans-epithelial Na^+ absorption, anion secretion stimulated via increased cAMP is evident in short-circuit conditions (Husted & Stokes, 1996; Green *et al.* 1996). Hyperosmolarity, typical of the inner medulla, is reported to have no effect (Husted & Stokes, 1996) or to reduce (but not abolish) transepithelial anion secretion by IMCD, despite reducing Na^+ absorption (Husted & Stokes, 1996; Green *et al.* 1996).

CFTR expression occurs in all segments of the rat nephron (Morales *et al.* 1996). In the IMCD there is expression of both full-length CFTR and a truncated isoform (Morales *et al.* 1996). The functional co-expression of CFTR together with Ca^{2+}-activated Cl^- conductance in mouse IMCD provides a rationale for understanding the absence of profound renal deficit in cystic fibrosis. Clarke *et al.* (1994) have hypothesised that severity of deficit due to defective CFTR in different organs correlates with expression of a Ca^{2+}-mediated apical epithelial Cl^- conductance. As in transgenic CF mouse pancreas (Clarke *et al.* 1994; Gray *et al.* 1995; Winpenny *et al.* 1995), it is likely that Ca^{2+}-activated Cl^- conductance can functionally compensate for loss of CFTR activity in humans.

Kunzelmann *et al.* (1997) have suggested that activation of human CFTR co-expressed in *Xenopus* oocytes inhibits the activation of endogenous Ca^{2+}-activated Cl^- currents. The data reported here for mIMCD-K2 cells partially support these findings since a small but significant reduction in the magnitude of Ca^{2+}-activated Cl^- conductance is observed upon CFTR activation. The marked absence of synergism between cAMP and Ca^{2+} stimuli noted here in epithelial layers most likely represents the limiting ability of baso-lateral anion transfer and/or K^+ conductance.

The extent of renal epithelial expression of Ca^{2+}-activated Cl^- conductance is unknown. A Ca^{2+}-activated Cl^- conductance has been described in mouse M1 cortical collecting duct cells (Meyer & Korbmacher, 1996), in primary cultures of rabbit proximal tubule cells and in distal bright convoluted tubule cells (Rubera *et al.* 1998) suggesting that expression is not restricted to the inner medulla. Clearly more work is required to map mCLCA1 expression along the nephron together with epithelial Na^+ and Cl^- channels to provide a framework to define regulatory interactions.

Altschul, S. F., Madden, T. L., Schaffer, A. A., Zhang, J. Z. Z., Miller, W. & Lipman, D. J. (1997). 'Gapped BLAST and PSI-BLAST: a new generation of protein database search programs'. *Nucleic Acids Research* **25**, 3389–3402.

Anderson, M. P. & Welsh, M. J. (1991). Calcium and cAMP activate different chloride channels in the apical membrane of normal and cystic fibrosis epithelia. *Proceedings of the National Academy of Sciences of the USA* **88**, 6003–6007.

Boese, S. H., Glanville, M., Gray, M. A. & Simmons, N. L. (1999*a*). A Ca^{2+}-activated Cl^- conductance is expressed at the apical membrane of mouse renal inner medullary collecting duct cells (mIMCD-K2). *Journal of Physiology* **517.P**, 66*P*.

Boese, S. H., Simmons, N. L. & Gray, M. A. (1999*b*). ATP and forskolin stimulate transepithelial Cl^- secretion in mouse renal inner medullary collecting duct cells (mIMCD-K2) by activation of distinct Cl^- conductances. *Journal of Physiology* **515.P**, 162*P*.

Boese, S. H., Wehner, F. & Kinne, R. K. (1996). Taurine permeation through swelling-activated anion conductance in rat IMCD cells in primary culture. *American Journal of Physiology* **271**, F498–501.

Brown, C. D. A., Lang, T. F. & Simmons, N. L. (1995). Characterisation of a purinoreceptor coupled to intracellular Ca^{2+} mobilisation in an inner medullary collecting duct cell line (IMCD3). *Japanese Journal of Physiology* **45**, suppl. 2, S38.

Clapp, W. L., Madsen, K. M., Veralnder, J. W. & Tisher, C. C. (1989). Morphologic heterogeneity along the rat inner medullary collecting duct. *Laboratory Investigations* **60**, 219–227.

Clarke, L. L., Grubb, B. R., Yankaskas, J. R., Cotton, C. U., McKenzie, A. & Boucher, R. C. (1994). Relationship of a non-cystic fibrosis transmembrane conductance regulator-mediated chloride conductance to organ-level disease in CFTR (−/−) mice. *Proceedings of the National Academy of Sciences of the USA* **91**, 479–483.

Cunningham, S. A., Awayda, M. S., Bubien, J. K., Ismailov, I. I., Arrate, M. P., Berdiev, B. K., Benos, D. J. & Fuller, C. M. (1995). Cloning of an epithelial chloride channel from bovine trachea. *Journal of Biological Chemistry* **270**, 31016–31026.

Ecelberger, C. A., Maeda, Y., Gibson, C. C. & Knepper, M. A. (1994). Extracellular ATP increases intracellular calcium in rat terminal collecting duct via a nucleotide receptor. *American Journal of Physiology* **267**, F998–1006.

Evans, M. G. & Marty, A. (1986). Calcium-dependent chloride currents in isolated cells from rat lacrimal glands. *Journal of Physiology* **378**, 437–460.

Gandhi, R., Elble, R. C., Gruber, A. D., Schreur, K. D., Ji, H. L., Fuller, C. M. & Pauli, B. U. (1998). Molecular and functional characterisation of a calcium-sensitive chloride channel from mouse lung. *Journal of Biological Chemistry* **273**, 32096–32101.

Gray, M. A., Winpenny, J. P., Porteus, D. J., Dorin, J. R. & Argent, B. E. (1994). CFTR and calcium-activated chloride currents in pancreatic duct cells of a transgenic CF mouse. *American Journal of Physiology* **266**, C213–221.

Green, R. B., Slattery, M. J., Gianferrari, E., Kizer, N. L., McCoy, D. E. & Stanton, B. A. (1996). Hyperosmolarity inhibits sodium absorption and chloride secretion in mIMCD-K2 cells. *American Journal of Physiology* **271**, F1248–1254.

Gruber, A. D., Gandhi, R. & Pauli, B. U. (1998). The murine calcium-sensitive chloride channel (mCACC) is widely expressed in secretory epithelia and other select tissues. *Histochemistry and Cell Biology* **110**, 43–49.

Hamill, O. P., Marty, A., Neher, E., Sakmann, B. & Sigworth, F. J. (1981). Improved patch-clamp techniques for high-resolution current recording from cells and cell-free membrane patches. *Pflügers Archiv* **391**, 85–100.

Husted, R. F. & Stokes, J. B. (1996). Separate regulation of Na and anion transport by IMCD: location, aldosterone, hypertonicity, TGF-beta1 and cAMP. *American Journal of Physiology* **271**, F433–439.

Husted, R. F., Volk, K. A., Sigmund, R. D. & Stokes, J. B. (1995). Anion secretion by the inner medullary collecting duct. *Journal of Clinical Investigation* **95**, 644–650.

Husted, R. F., Zhang, C. & Stokes, J. B. (1998). Concerted actions of IL-1beta inhibit Na absorption and stimulate anion secretion by IMCD cells. *American Journal of Physiology* **275**, F946–954.

King, N., Colledge, W. H., Ratcliff, R., Evans, M. J. & Simmons, N. L. (1997). The intrinsic Cl conductance of mouse kidney cortex brush-border membrane vesicles is not related to CFTR. *Pflügers Archiv* **434**, 575–580.

Kizer, N. L., Lewis, B. & Stanton, B. A. (1995). Electrogenic sodium absorption and chloride secretion by an inner medullary collecting duct cell line (mIMCD-K2). *American Journal of Physiology* **268**, F347–355.

Kunzelmann, K., Mall, M., Briel, M., Hipper, A., Nitschke, R., Ricken, S. & Greger, R. (1997). The cystic fibrosis transmembrane conductance regulator attenuates the endogenous Ca^{2+}-activated Cl^- conductance of *Xenopus* oocytes. *Pflügers Archiv* **435**, 178–181.

Letz, B. & Korbmacher, C. (1997). cAMP stimulates CFTR-like Cl channels and inhibits amiloride-sensitive Na channels in mouse CCD cells. *American Journal of Physiology* **272**, C657–666.

Meyer, K. & Korbmacher, C. (1996). Cell swelling activates ATP-dependent voltage gated chloride channels in M1 mouse cortical collecting duct cells. *Journal of General Physiology* **108**, 177–193.

Morales, M. M., Carroll, T. P., Morita, T., Schweibert, E. M., Devuyst, O., Wilson, P. D., Lopes, A. G., Stanton, B. A., Dietz, H. C., Cutting, G. R. & Guggino, W. B. (1996). Both the wild-type and functional isoform of CFTR are expressed in kidney. *American Journal of Physiology* **270**, F1038–1048.

Obermuller, N., Gretz, N., Kriz, W., Reilly, R. F. & Witzgall, R. (1998). The swelling-activated chloride channel CLC2, the chloride channel CLC-3, and CLC-5, a chloride channel mutated in kidney stone disease, are expressed in distinct subpopulations of renal epithelial cells. *Journal of Clinical Investigation* **101**, 635–642.

Paulmichl, M., Li, Y., Wickman, K., Ackermann, M., Peralta, E. & Clapham, D. (1992). New mammalian Cl^- channel identified by expression cloning. *Nature* **356**, 238–241.

Poncet, V., Tauc, M., Bidet, M. & Poujeol, P. (1994). Chloride channels in apical membrane of primary cultures of rabbit distal bright convoluted tubule. *American Journal of Physiology* **266**, F543–553.

Rocha, A. S. & Kudo, L. H. (1990*a*). Atrial peptide and cGMP effects on NaCl transport in inner medullary collecting duct. *American Journal of Physiology* **259**, F265–268.

Rocha, A. S. & Kudo, L. H. (1990*b*). Factors governing sodium and chloride transport across the inner medullary collecting duct. *Kidney International* **38**, 654–667.

Romio, L., Musante, L., Cinti, R., Seri, M., Moran, O., Zegarra-Moran, O. & Galietta, L. J. V. (1999). Characterisation of a murine gene homologous to the bovine CACC chloride channel. *Gene* **228**, 181–188.

Rubera, I., Tauc, M., Bidet, M., Poujeol, C., Cuiller, B., Watrin, A., Touret, N. & Poujeol, P. (1998). Chloride currents in primary cultures of rabbit proximal and distal convoluted tubules. *American Journal of Physiology* **275**, F651–663.

Sansom, S. C., Mougouris, T., Ono, S. & Dubose, T. D. (1994). ATP-sensitive K^+-selective channels of inner medullary collecting duct cells. *American Journal of Physiology* **267**, F489–496.

Schwiebert, E. M., Lopes, A. G. & Guggino, W. B. (1994). Chloride channels along the nephron. *Current Topics in Membranes* **42**, 265–315.

Simmons, N. L. (1991). The effect of hypo-osmolarity upon transepithelial ion transport in cultured renal epithelial layers (MDCK). *Pflügers Archiv* **419**, 572–579.

Simmons, N. L. (1992). Acetylcholine and kinin augmentation of Cl^- secretion by prostaglandin E_1 in a canine renal epithelial cell line (MDCK). *Journal of Physiology* **447**, 1–15.

Simmons, N. L. (1993). Renal epithelial Cl^- secretion. *Experimental Physiology* **78**, 117–137.

Terada, Y., Moriyama, T., Martin, B. M., Knepper, M. A. & Garcia-Perez, A. (1991). RT-PCR microlocalisation of mRNA for guanylyl cyclase-coupled ANF receptor in rat kidney. *American Journal of Physiology* **261**, F1080–1087.

Thwaites, D. T., Ford, D., Glanville, M. & Simmons, N. L. (1999). H^+/solute intracellular acidification leads to selective activation of apical Na^+/H^+exchange in human intestinal epithelial cells. *Journal of Clinical Investigation* **104**, 629–635.

Uchida, S., Sasaki, S., Furukawa, T., Hiraoka, M., Imai, T., Hirata, Y. & Marumo, F. (1993). Molecular cloning of a chloride channel that is regulated by dehydration and expressed predominantly in kidney medulla. *Journal of Biological Chemistry* **268**, 3821–3824.

Uchida, S., Sasaki, S., Nitta, K., Uchida, K., Horita, S., Nihei, H. & Marumo, F. (1995). Localisation and functional characterisation of rat kidney-specific chloride channel ClC-K1. *Journal of Clinical Investigation* **95**, 104–113.

Vandorpe, D. H., Ciampolillo, F., Green, R. B. & Stanton, B. A. (1997). Cyclic nucleotide-gated cation channels mediate sodium absorption by IMCD (mIMCD-K2) cells. *American Journal of Physiology* **272**, C901–910.

Vandorpe, D., Kizer, N., Ciampollilo, F., Moyer, B., Karlson, K., Guggino, W. B. & Stanton, B. A. (1995). CFTR mediates electrogenic chloride secretion in mouse inner medullary collecting duct (mIMCD-K2) cells. *American Journal of Physiology* **269**, C683–689.

Walker, D., Thwaites, D. T., Simmons, N. L., Gilbert, H. J. & Hirst, B. H. (1998). Substrate upregulation of the human intestinal peptide transporter hPepT1. *Journal of Physiology* **507**, 697–706.

Winpenny, J. P., Harris, A., Hollingsworth, M. A., Argent, B. E. & Gray, M. A. (1998). Calcium-activated chloride conductance in a pancreatic adenocarcinoma of ductal origin (HPAF) and in freshly isolated human pancreatic duct cells. *Pflügers Archiv* **435**, 796–803.

Winpenny, J. P., Verdon, B., McAlroy, H. L., Colledge, W. H., Ratcliff, R., Evans, M. J., Gray, M. A. & Argent, B. E. (1995). Calcium-activated chloride conductance is not increased in pancreatic duct cells of CF mice. *Pflügers Archiv* **430**, 26–36.

Zeidel, M. L. (1993). Hormonal regulation of inner medullary collecting duct sodium transport. *American Journal of Physiology* **265**, F159–173.

Acknowledgements

This work was supported by a grant from the Wellcome Trust. We thank C. Ward for skilled technical assistance.

Corresponding author

N. L. Simmons: Department of Physiological Sciences, Medical School, Framlington Place, University of Newcastle upon Tyne, Newcastle upon Tyne NE2 4HH, UK.

Email: n.l.simmons@ncl.ac.uk